Theoretical studies of the stability of ordered A_8B compounds

Z. W. Lu and Barry M. Klein

Department of Physics, University of California, Davis, California 95616

(Received 5 May 1994)

Ten out of 27 possible A_8B (prototype Pt_8Ti) compounds, where A =Ni,Pd,Pt, and B are IVA, VA, and VIA elements, have been experimentally observed. For these compounds to be thermodynamically stable, their $T = 0$ formation energy ΔH must be negative, and ΔH must lie below the tie line connecting neighboring ground states. Using the first-principles total-energy approach as implemented in the linearized augmented-plane-wave LAPW method, we have calculated the $T = 0$ ΔH of $(Ni,Pd,Pt)_8B$ (B =V, Cr, Mo, and W) and of their neighboring known (or suspected) ground-state structures. We find that (i) $\Delta H < 0$ for these compounds except for Pd_8Cr, for which $\Delta H > 0$; (ii) $\Delta H(A_8B)$ lies below the tie line connecting the neighboring known (or suspected) ground states and the end point (pure element). These A_8B structures appear to be true, stable ground states for these systems. We further elucidate the stability or instability of these systems in terms of their underlying electronic structures, and also calculate their electron-phonon interactions. We conclude that these materials are unlikely to be superconductors.

I. INTRODUCTION

Ten out of 27 possible A_8B (prototype Pt_8Ti) compounds, where A are the face-centered-cubic (fcc) VIIIA late transition metals (Ni, Pd, and Pt) and B are the hexagonal close-packed (hcp) IVA (Ti, Zr, and Hf), body-centered-cubic (bcc) VA (V, Nb, and Ta), and VIA (Cr, Mo, and W) early transition metals, have been experimentally observed.[1] These experimentally identified compounds[2-12] are summarized in Table I by the symbols √. The crystallographic structure of the A_8B is illustrated in Fig. 1. This structure has a body-centered-tetragonal Bravais lattice derived from the underlying face-centered-cubic lattice. While the Pt_8B phases nucleate and grow with normal annealing treatments at high temperatures, Ni_8B and Pd_8B phases all require excess vacancies for the ordering reaction to proceed at experimentally accessible rates.[1] Many of these ordered compounds[7,8,10,11] have been observed only under the condition of charged particle irradiation. However, experimental evidence[1] suggests that these observed A_8B phases are thermodynamically stable.

The question of whether a crystallographic configuration σ for a binary system is a stable ground state or not can be theoretically addressed by calculating its $T = 0$ formation energy, $\Delta H(\sigma)$, defined as

$$\Delta H(\sigma) = E(\sigma, V_\sigma) - [(1 - x)E_A(V_A) + xE_B(V_B)] . \quad (1)$$

Here, $\Delta H(\sigma)$ is taken with respect to the energy of equivalent amounts of the constituent solids A and B at their respective equilibrium volumes V_A and V_B. In order for σ to be a ground state, it has to satisfy the following conditions: (i) Its formation energy must be negative, $\Delta H(\sigma) < 0$; i.e., the energy of the ordered configuration is lower than the energy of a linear combination of the equivalent amounts of equilibrium A and B (phase separation). (ii) $\Delta H(\sigma)$ is the lowest among all the structures with the same atomic composition as the configuration σ. (iii) $\Delta H(\sigma)$ has to lie below the tie line connecting the neighboring ground states in the energy versus composition diagram.[13] Let σ, α, and β be three configurations with concentration of B atoms x_σ, x_α, and x_β in the order $x_\alpha \leq x_\sigma \leq x_\beta$. If $\Delta H(\sigma)$ is larger than the linear average of $\Delta H(\alpha)$ and $\Delta H(\beta)$, that is,

$$\Delta H(\sigma) > \frac{x_\sigma - x_\beta}{x_\alpha - x_\beta}\Delta H(\alpha) + \frac{x_\sigma - x_\alpha}{x_\beta - x_\alpha}\Delta H(\beta), \quad (2)$$

TABLE I. This table indicates the experimental observed (by the symbol √) Ni_8B, Pd_8B, and Pt_8B (where B=Ti, Zr, Hf, V, Nb, Ta, Cr, Mo, and W) phases in the $I4/mmm$, $tI18$ bct structure.

	Ti	Zr	Hf	V	Nb	Ta	Cr	Mo	W
	hcp	hcp	hcp	bcc	bcc	bcc	bcc	bcc	bcc
Ni (fcc)				√[a]	√[a]	√[a]		√[b]	
Pd (fcc)				√[c]				√[d]	√[e]
Pt (fcc)	√[f]	√[g]		√[h]					

[a]References 4–6.
[b]Reference 10.
[c]References 8, 12.
[d]Reference 11.
[e]Reference 7.
[f]Reference 2.
[g]Reference 3.
[h]Reference 9.

then configuration σ does not belong to the ground state because a mixture of the equilibrium phases α and β would have a lower energy.

Here, we will theoretically investigate the thermodynamic stabilities of some of these A_8B phases using an accurate, first-principles electronic structure method. We choose to study 12 A_8B systems, for which $A=$ VIIIA (Ni, Pd, and Pt) and B = VIA (Cr, Mo, and W) as well as one VA element V. While (Ni,Pd,Pt)$_8$V are known to form ordered A_8B compounds, the stabilities of the A_8B compounds among many members of the matrix between VIIIA and VIA are not certain. Hence, we will test the ability of the local-density-based[14] total-energy method to verify the stability of the (Ni,Pd,Pt)$_8$V systems, and further predict the stabilities of nine other A_8B compounds. Specifically, we will (a) calculate the $T = 0$ formation energy ΔH for the A_8B phases and neighboring known or suspected ground states; (b) compare the resulting $\Delta H(A_8B)$ with that of neighboring known or suspected ground states, for 12 A_8B systems; (c) establish a chemical trend for $\Delta H(A_8B)$, and analyze the stability and instability of these systems in terms of their underlying electronic structures; (d) calculate the electron-phonon interaction for the A_8V compounds and estimate their superconducting transition temperatures; and (e) review the recent literature results on the ability of a "generalized Ising model" to predict the A_8B as a ground state in Ni$_8$V,[15] Pd$_8$V,[16] and Pt$_8$V.[16] Finally we will briefly summarize the findings of this work.

II. METHOD OF CALCULATION

We calculate the total energies of the periodic crystals in the local-density approximation (LDA).[14] We have used the Wigner[17] exchange-correlation potential. The LDA equations are solved self-consistently by the linearized augmented-plane-wave (LAPW) method.[18] The core states are treated fully relativistically, while the valence states are treated semirelativistically (without spin-

orbit interaction). No shape approximation is made for either the potential or the charge density. Inside the muffin-tin spheres, the nonspherical charge density and potential are expanded in terms of lattice harmonics of angular momentum $l \leq 8$. A basis set of about ~ 90 LAPW's/atom are used. The Brillouin zone (BZ) integration is performed using the special k-point method,[19] with 20–200 k points in the irreducible BZ (depending on the structure). We have also calculated the total energies of the elemental metals as a function of volume for a number of points around the equilibrium volume, extracting their equilibrium lattice parameters, bulk moduli, and pressure derivatives using the Murnaghan equation of state.[20] For ordered compounds, we only minimize the total energy as a function of volume.[21] The convergence error for the total energy is estimated to be approximately 10 meV/atom.

III. STRUCTURAL PROPERTIES FOR THE ELEMENTS

Table II compares the calculated and experimental[22,23] equilibrium lattice parameters a_0, bulk moduli B_0, and their pressure derivatives B_0' for the elemental metals. The calculated lattice parameters are within 2.2% of the measured values, with the largest differences occurring for the $3d$ metals Cr, V, and Ni, where the LDA underestimates the lattice parameters by 2.2%, 2.1%, and 1.9%, respectively. The largest differences in bulk moduli between calculation and experiment also occur for the $3d$ metals (by as much as 44% in Cr), partly due to the fact that the LDA-calculated lattice parameters are smaller than experiment. Extrapolating the calculated, equilibrium bulk moduli to the values at the experimental lattice parameters using the Murnaghan equation of state[20] leads to much smaller discrepancies (i.e., only 13% for Cr). Table II also gives the structural information for V, Cr, Mo, and W in the fcc structure, as well as the energy differences between the bcc and fcc structures

TABLE II. Comparison of calculated and experimental equilibrium lattice constants a_0 (Å), bulk moduli B_0 (GPa), and their pressure derivatives B_0' for solid Ni, Pd, Pt, V, Cr, Mo, and W. We also give the equilibrium total-energy difference between the bcc and fcc structures [$\delta E_0 = E_0(\text{bcc}) - E_0(\text{fcc})$ in units of meV/atom].

Elemental metal	Structure	a_0 Calc.	a_0 Expt.[a]	B_0 Calc.	B_0 Expt.[b]	B_0' Calc.	δE_0 Calc.
Ni	fcc	3.458	3.524	248.9	186	4.77	
Pd	fcc	3.882	3.887	211.1	180.8	5.28	
Pt	fcc	3.935	3.924	287.0	278.3	5.28	
V	bcc	2.966	3.030	185.7	161.9	2.57	
V	fcc	3.779		184.2		4.50	265.2
Cr	bcc	2.822	2.884	273.2	190.1	3.69	
Cr	fcc	3.590		257.1		3.54	400.1
Mo	bcc	3.146	3.145	263.5	272.5	3.74	
Mo	fcc	3.986		246.1		2.85	431.3
W	bcc	3.172	3.165	304.9	323.2	3.13	
W	fcc	4.024		286.1		3.34	477.2

[a]Reference 22, room temperature data.
[b]Reference 23.

$\delta E_0 = E_0(\text{fcc}) - E_0(\text{bcc})$. One notices that the transition from bcc to fcc becomes energetically more difficult along the V $\to$ Cr $\to$ Mo $\to$ W sequence.

IV. STRUCTURAL PROPERTIES FOR THE ORDERED A_8B COMPOUNDS

Figure 1 depicts the A_8B structure. It has the body-centered-tetragonal Bravais lattice (space group $I4/mmm$ and Pearson symbol $tI18$) with lattice vectors

$$\mathbf{a} = 1.5a_0 \,\hat{x} + 0.0c_0 \,\hat{y} + 1.5a_0 \,\hat{z},$$
$$\mathbf{b} = 1.5a_0 \,\hat{x} + 0.0c_0 \,\hat{y} - 1.5a_0 \,\hat{z}, \qquad (3)$$
$$\mathbf{c} = 1.5a_0 \,\hat{x} + 0.5c_0 \,\hat{y} + 0.0a_0 \,\hat{z},$$

where a_0 and c_0 are tetragonal lattice constants. There are three types of inequivalent atoms in the unit cell, with the atomic positions of these atoms in Cartesian coordinates given by

$$A^{(1)} = 0.5a_0 \,\hat{x} + 0.0c_0 \,\hat{y} + 0.5a_0 \,\hat{z},$$
$$A^{(2)} = 1.0a_0 \,\hat{x} + 0.5c_0 \,\hat{y} + 1.5a_0 \,\hat{z}, \qquad (4)$$
$$B^{(1)} = 0.0a_0 \,\hat{x} + 0.0c_0 \,\hat{y} + 0.0a_0 \,\hat{z},$$

where both $A^{(1)}$ type and $A^{(2)}$ type have four equivalent atoms in the unit cell. Since available experimental data[1] suggest that $a_0 \approx c_0$, we assume $a_0 = c_0$ in the total-energy minimization. Table III shows our calculated equilibrium lattice parameter ($T = 0$ K) a_{calc} along with the experimental values.[1] The calculated lattice parameters agree well with experiment ($\leq 1.1\%$), contracting by $\lesssim 0.5\%$ (except for Pt-Cr, for which it expands by 0.2%) with respect to the values obtained using Vegard's rule,

$$\bar{a} = \left[\frac{4(8V_A + V_B)}{9} \right]^{\frac{1}{3}}, \qquad (5)$$

where V_A and V_B are the equilibrium volumes in the parent fcc structures.
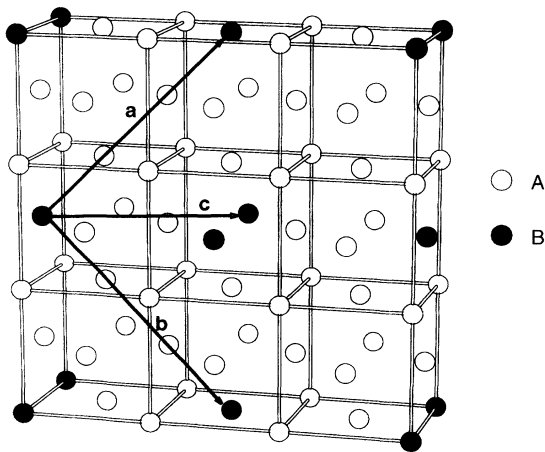
FIG. 1. The crystallographic structure of the A_8B phase. The Bravais vectors are represented by the arrowed lines. The space group of the A_8B structure is $I4/mmm$; its Pearson symbol is $tI18$.

TABLE III. The LAPW-calculated cubic lattice parameters (a) compared with $\bar{a} = [(8V_A + V_B)4/9]^{1/3}$, and available experimental values for A_8B (where $A=$ fcc Ni, Pd, and Pt, while $B=$ fcc V, Cr, Mo, and W) phases in the $I4/mmm$, $tI18$ bct structure.

	Ni-V	Pd-V	Pt-V
a_{calc}	3.474	3.851	3.909
$\bar{a}$	3.497	3.871	3.918
a_{expt}			3.866
	Ni-Cr	Pd-Cr	Pt-Cr
a_{calc}	3.463	3.848	3.903
$\bar{a}$	3.473	3.852	3.900
	Ni-Mo	Pd-Mo	Pt-Mo
a_{calc}	3.519	3.878	3.933
$\bar{a}$	3.525	3.894	3.941
a_{expt}		3.883	
	Ni-W	Pd-W	Pt-W
a_{calc}	3.524	3.879	3.935
$\bar{a}$	3.530	3.898	3.945
a_{expt}		3.887	

V. FORMATION ENERGIES OF THE ORDERED A_8B COMPOUNDS

Table IV gives the LAPW-calculated formation energies $\Delta H(A_8B)$ for 12 A_8B compounds, where $A =$ Ni, Pd, and Pt, while $B =$ V, Cr, Mo, and W. One immediately notices that $\Delta H(A_8B) < 0$ for all compounds, except for Pd$_8$Cr for which $\Delta H(\text{Pd}_8\text{Cr}) > 0$. Hence, all of the A_8B compounds studied here (except Pd$_8$Cr) are stable with respect to phase separation into their equilibrium constituents, i.e., fcc A (Ni, Pd, and Pt) and bcc B (V, Cr, Mo, and W). Figure 2(a) depicts $\Delta H(A_8B)$ for these compounds. We notice the following chemical trends: (i) For $A =$ Ni, Pd, and Pt, the following relation holds: $\Delta H(A_8\text{Cr}) > \Delta H(A_8\text{Mo}) > \Delta H(A_8\text{W}) > \Delta H(A_8\text{V})$; (ii) for $B =$ Mo, W, and V, $\Delta H(\text{Ni}_8B) \approx \Delta H(\text{Pd}_8B)$, while Pt$_8B$ is much more stable than either Ni$_8B$ or Pd$_8B$. In the case of $B =$ Cr, $\Delta H(\text{Ni}_8\text{Cr}) \approx \Delta H(\text{Pt}_8\text{Cr})$, while Pd$_8$Cr is the only compound that is found to be unstable with respect to a phase separation into equilibrium fcc Pd and bcc Cr. In Sec. VII we will further address these chemical trends in terms of their underlying electronic structures.

VI. RELATIVE STABILITIES OF THE A_8B COMPOUNDS WITH NEIGHBORING GROUND STATES

While the compounds studied here (except Pd$_8$Cr) are stable [$\Delta H(A_8B) < 0$] with respect to phase separation into equivalent amounts of their equilibrium constituents A and B, we have yet to answer the question of whether they are stable with respect to phase separation into equivalent amounts of their neighboring, equilibrium ground states [as in Eq. (2)]. Table IV gives the calculated formation energies of the neighboring, known or suspected, ground states $\Delta H(\beta)$ for $x > \frac{1}{9}$, while for $x < \frac{1}{9}$, we take α as the end point [i.e., fcc Ni, Pd, and

TABLE IV. The LAPW-calculated formation energies ΔH (in meV/atom) for Ni_8X, Pd_8X, and Pt_8X (where X=V, Cr, Mo, and W) phases in the $I4/mmm$, $tI18$ bct structure. We give the formation energies $\Delta H(\beta)$ of neighboring, known or suspected, ground states for these alloys as well as the values of $\Delta H(A_8B) - \Delta E(\frac{1}{9})$, where $\Delta E(\frac{1}{9}) = \Delta H(\beta)/9x_\beta$.

	Structure	Ni-V	Pd-V	Pt-V
$\Delta H(A_8B)$	A_8B $(x = \frac{1}{9})$	−189.4	−183.7	−256.8
$\Delta E_{VD}(\frac{1}{9})$		100.7	37.3	42.6
$\varepsilon_{CE}(A_8B)$		−290.1	−221.0	−299.4
$\Delta H(\beta)$	DO_{22} $(x = \frac{1}{4})$	−313.3	−283.9	−471.4
$\Delta H(A_8B) - \Delta E(\frac{1}{9})$		−50.2	−57.5	−47.3
		Ni-Cr	**Pd-Cr**	**Pt-Cr**
$\Delta H(A_8B)$	A_8B $(x = \frac{1}{9})$	−66.0	4.2	−63.1
$\Delta E_{VD}(\frac{1}{9})$		57.5	91.1	109.8
$\varepsilon_{CE}(A_8B)$		−123.5	−86.9	−172.9
$\Delta H(\beta)$	$L1_2$ $(x = \frac{1}{4})$		120.8	−73.4
$\Delta H(\beta)$	Pt_2Mo $(x = \frac{1}{3})$	−93.1		
$\Delta H(A_8B) - \Delta E(\frac{1}{9})$		−35.0		−30.5
		Ni-Mo	**Pd-Mo**	**Pt-Mo**
$\Delta H(A_8B)$	A_8B $(x = \frac{1}{9})$	−107.1	−116.2	−174.2
$\Delta E_{VD}(\frac{1}{9})$		281.3	57.2	50.1
$\varepsilon_{CE}(A_8B)$		−388.4	−173.4	−224.3
$\Delta H(\beta)$	Ni_4Mo $(x = \frac{1}{5})$	−144.3		
$\Delta H(\beta)$	Pt_2Mo $(x = \frac{1}{3})$		−161.8	−390.1
$\Delta H(A_8B) - \Delta E(\frac{1}{9})$		−26.9	−62.2	−44.2
		Ni-W	**Pd-W**	**Pt-W**
$\Delta H(A_8B)$	A_8B $(x = \frac{1}{9})$	−131.3	−139.5	−189.1
$\Delta E_{VD}(\frac{1}{9})$		392.9	73.5	60.5
$\varepsilon_{CE}(A_8B)$		−524.2	−213.0	−249.6
$\Delta H(\beta)$	Ni_4Mo $(x = \frac{1}{5})$	−176.8	−150.2	−285.9
$\Delta H(A_8B) - \Delta E(\frac{1}{9})$		−33.1	−56.1	−30.3

Pt, $x_\alpha = 0$ and $\Delta H(\alpha) = 0$]. Hence, with the right-hand side of inequality (2) defined as

$$\Delta E\left(\frac{1}{9}\right) = \frac{\Delta H(\beta)}{9x_\beta} , \qquad (6)$$

we can compare $\Delta E(\frac{1}{9})$ with $\Delta H(A_8B)$ to determine whether the A_8B structures are stable $[\Delta H(A_8B) < \Delta E(\frac{1}{9})]$ with respect to phase separation into the neighboring ground state α and the fcc end point. Table IV gives the formation energies of the neighboring ground state $\Delta H(\beta)$ as well as the corresponding $\Delta H(A_8B) - \Delta E(\frac{1}{9})$. The negative sign of $\Delta H(A_8B) - \Delta E(\frac{1}{9})$ reveals that these A_8B phases are indeed stable with respect to phase separation into the neighboring ground state β and the fcc end point. We will next address this issue in more detail.

A. Vanadium systems

The A_8V phases are the only systems that have been observed experimentally for all three A elements, Ni, Pd, and Pt. The observed phase diagrams[24] for the vanadium alloys show that there are ground states at $x = \frac{1}{4}$ and these A_3V $(A = $ Ni, Pd, and Pt) phases all crystallize in the DO_{22} structure.[25-29] These DO_{22} phases are found to be stable: Their formation energies are −313.3, −283.9, and −471.4 meV/atom for Ni_3V, Pd_3V, and Pt_3V, respectively, and their corresponding $\Delta E(\frac{1}{9})$ [Eq. (6)] values are −139.2, −126.2, −209.5 meV/atom as shown in Table IV. We find that the formation energies
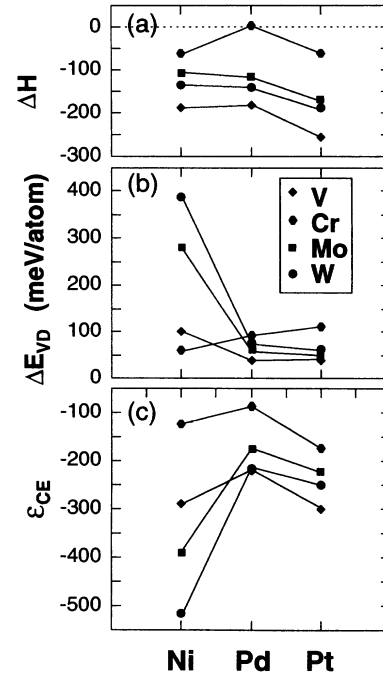
FIG. 2. The figure shows the LAPW-calculated (a) formation energies ΔH (in meV/atom) for the A_8B structures. We also decompose ΔH according to Eq. (8) into (b) "volume deformation" ΔE_{VD}, and (c) "charge exchange" ε_{CE} energies. The quantities for A_8V, A_8Cr, A_8Mo, and A_8W $(A = $ Ni, Pd, and Pt) are denoted by the solid diamonds, hexagons, squares, and circles, respectively. These symbols are connected by straight lines to guide the eyes.

$\Delta H(A_8 V)$ are *lower* in energy than their corresponding $\Delta E(\frac{1}{9})$ by ~ 50 meV/atom. Therefore, our calculations show that these $A_8 V$ phases are indeed stable with respect to phase separating into their neighboring equilibrium ground states, in agreement with the fact that the $Ni_8 V$, $Pd_8 V$, and $Pt_8 V$ phases are observed[1] experimentally.

B. Chromium systems

The observed phase diagrams[24] for the chromium alloys are less well established than for the vanadium systems. For Ni-Cr, on the Ni-rich side, the existence of the ordered ground state $Ni_2 Cr$ (prototype $MoPt_2$) is well established, and the *calculated* formation energy for $Ni_2 Cr$ in the $MoPt_2$ structure is stable (-93.1 meV/atom). The calculated $\Delta H(Ni_8 Cr)$ (-66.0 meV/atom) is 35.0 meV/atom below the value of $\Delta E(\frac{1}{9})$ (-31.0 meV/atom). For Pt-Cr, on the Pt-rich side, there exists an ordered phase with the $L1_2$ structure at $x = \frac{1}{4}$. This ordered structure is found to be theoretically stable with the calculated $\Delta H(Pt_3 Cr) = -73.4$ meV/atom. The calculated $\Delta H(Pt_8 Cr) = -63.1$ meV/atom is thus -30.5 meV/atom below the value of $\Delta E(\frac{1}{9}) = -32.6$ meV/atom, and hence $Pt_8 Cr$ is stable. $Pd_8 Cr$ is the only system that is found to be marginally unstable against phase separation into equilibrium fcc Ni and bcc Cr [$\Delta H(Pd_8 Cr) = +4.2$ meV/atom]. The assessed phase diagram indicates the possible existence of an ordered $L1_2$-like structure (however, at the off-stoichiometric $Pd_3 Cr_2$ rather than at $Pd_3 Cr$). Our calculated formation energy for stoichiometric $Pd_3 Cr$ in the $L1_2$ structure is positive ($+120.8$ meV/atom); hence this structure is unstable with respect to phase separation into equivalent amounts of equilibrium fcc Pd and bcc Cr, as is $Pd_8 Cr$ in the $Pt_8 Ti$-type structure. This is because the Pd-Cr system has a relatively large elastic strain energy and a relatively weak chemical attraction between Pd and Cr.

C. Molybdenum systems

The observed phase diagrams[24] for the molybdenum alloys show ordered ground states at $x = \frac{1}{5}$ for Ni-Mo and at $x = \frac{1}{3}$ for both Pd-Mo and Pt-Mo. Interestingly, these ordered molybdenum compounds belong to the $\langle 1\frac{1}{2} 0 \rangle$ family of structures; i.e., they can be characterized by the same reciprocal wave vector $\mathbf{k} = \langle 1\frac{1}{2} 0 \rangle$. The ordered $Ni_4 Mo$ structure (the prototype is itself $Ni_4 Mo$) is a superlattice along the [210] directions with four layers of Ni followed by one layer of Mo stacked along the [210] direction in the unit cell, while the $Pd_2 Mo$ and $Pt_2 Mo$ structures (the prototype $Pt_2 Mo$) are also superlattices along the [210] directions with two layers of Pd (Pt) followed by one layer of Mo stacks along the [210] direction in the unit cell. The calculated formation energies for these ordered structures are -144.3, -161.8, and -390.1 meV/atom for $Ni_4 Mo$, $Pd_2 Mo$, and $Pt_2 Mo$, respectively. The calculated formation energies for $Ni_8 Mo$, $Pd_8 Mo$, and $Pt_8 Mo$ are -107.1, -116.2, and -174.2 meV/atom,

respectively, which is 26.9, 62.2, and 44.2 meV/atom below their respective values of $\Delta E(\frac{1}{9})$. We confirm here the stabilities of the ordered $Ni_8 Mo$ and $Pd_8 Mo$ phases, as these phases are observed[1] experimentally. We further predict that the $Pt_8 Mo$ is stable as well.

D. Tungsten systems

For the tungsten systems, the phase diagrams[24] are relatively little explored especially for Pd-W and Pt-W: Only the high-temperature part of the phase diagram ($T > 1273$ K for Pd-W and $T > 1873$ K for Pt-W) are available. For Ni-W, the observed phase diagram shows that there is an ordered $Ni_4 W$ (prototype $Ni_4 Mo$) phase. We therefore assume that both $Pd_4 W$ and $Pt_4 Mo$ also have ordered $Ni_4 Mo$-type ground states. The calculated ΔH values in the $Ni_4 Mo$-type structure are -176.8, -150.2, -285.9 meV/atom for $Ni_4 W$, $Pd_4 W$, and $Pt_4 W$, respectively, while the $\Delta H(A_8 B)$ values are 33.1, 56.0, and 30.3 meV/atom *below* their respective values of $\Delta E(\frac{1}{9})$ [Eq. (6)] for the same sequence. The stability of the $Pd_8 W$ phase has been established experimentally; here we predict that both $Ni_8 W$ and $Pt_8 W$ are stable, too.

VII. ELECTRONIC ORIGINS OF THE STABILITIES OF $A_8 B$ COMPOUNDS

The formation energy $\Delta H(\sigma)$ in Eq. (1) can be partitioned into the following form:

$$
\begin{aligned}
\Delta H(\sigma) = &\{(1 - x)[E_A(V_\sigma) - E_A(V_A)] \\
&+ x[E_B(V_\sigma) - E_B(V_B)]\} \\
&+ \{E(\sigma, V_\sigma) - [(1 - x)E_A(V_\sigma) + x E_B(V_\sigma)]\} \cdot
\end{aligned}
$$
(7)

The first term in the curly brackets is the "volume deformation" elastic energy (positive definite) energy $\Delta E_{\mathrm{VD}}(V_\sigma)$, associated with "preparing" A and B by hydrostatically deforming the constituents $(1 - x)A + xB$ from their equilibrium volumes V_A and V_B to the final alloy volume $V = V_\sigma$. In the present case, we add an additional term $\delta E_0 = E_B(\mathrm{fcc}) - E_B(\mathrm{bcc})$, which is the energy change due to the underlying crystallographic structural transition, i.e., a phase transition from bcc to fcc for the B atoms. The second term is the energy change $\varepsilon_{\mathrm{CE}}$ associated with forming the alloy σ from $(1 - x)A + xB$ at the *fixed volume* V_σ. This term is labeled "chemical energy" since, unlike the first term, it describes $A - B$ interactions. It includes "charge exchange" and (nonhydrostatic) atomic relaxations (neglected here), and can be either negative (e.g., for all the compounds considered here) or positive (e.g., for the phase-separating Pd-Rh system). If the equilibrium volumes $V_\sigma(x)$ depend primarily on the composition x (either linearly or nonlinearly) and only weakly on the configuration σ, then the first term is a constant for all configurations σ [$\Delta E_{\mathrm{VD}}(V_\sigma) \equiv \Delta E_{\mathrm{VD}}(x)$], which can be ob-

tained easily (either performing direct LDA calculations on the constituents or using the fitted Murnaghan equation of state). Table IV gives the decomposed formation energy $\Delta H(A_8B)$ into

$$\Delta H(A_8B) = \Delta E_{\mathrm{VD}}\left(\frac{1}{9}\right) + \varepsilon_{\mathrm{CE}}(A_8B) \ , \qquad (8)$$

i.e., the "volume deformation" energy $\Delta E_{\mathrm{VD}}(x)$ (at $x = \frac{1}{9}$) and the "chemical energy" $\varepsilon_{\mathrm{CE}}(A_8B)$.

Figure 2(b) depicts $\Delta E_{\mathrm{VD}}(x)$. We notice the following trend: The volume deformation energies $\Delta E_{\mathrm{VD}}(\frac{1}{9})$ are on the order of 100 meV/atom except for Ni-Mo and Ni-W, for which the large volume mismatches between the constituents ($> 40\%$) result in the largest $\Delta E_{\mathrm{VD}}(\frac{1}{9})$ of 281.3 and 392.9 meV/atom, respectively. Pd-V and Pt-V have the smallest volume deformation energies of 37.3 and 42.6 meV/atom.

The "charge exchange" or "chemical energy" $\varepsilon_{\mathrm{CE}}(A_8B)$ defined in Eqs. (7) and (8) is attractive for all compounds studied here as illustrated in Fig. 2(c) and listed in Table IV. The chemical trend of $\varepsilon_{\mathrm{CE}}(A_8B)$ can be further discussed by using the "charge exchange" or "charge transfer" concept. Here, we define charge transfer as the difference in the amount of charge within the muffin-tin sphere radius in the compound and in the pure fcc environment at the same molar volume,

$$\Delta Q_l^{\mathrm{MT}} = Q_l^{\mathrm{MT}}(A_8B) - Q_l^{\mathrm{MT}}(\mathrm{fcc}) \ , \qquad (9)$$

where l denotes the angular momentum quantum number. Table V gives the values of ΔQ_l^{MT} for the A_8B phases (except for Ni-Mo and Ni-W for which the muffin-tin radii of Mo and W overlap in the elemental fcc form at the lattice constant of the respective A_8B phases). Com-

paring Fig. 2(c) and Table V, we notice the following.

(i) $\varepsilon_{\mathrm{CE}}(A_8B)$ are attractive, which loosely correlates with the substantial amount of charge transfer for these alloys.

(ii) Within the isoelectronic series of Pd_8B and Pt_8B, where $B = $ Cr, Mo, and W, $\varepsilon_{\mathrm{CE}}(A_8B)$ correlates with the amount of total charge transfer, i.e., $\varepsilon_{\mathrm{CE}}(A_8\mathrm{W}) < \varepsilon_{\mathrm{CE}}(A_8\mathrm{Mo}) < \varepsilon_{\mathrm{CE}}(A_8\mathrm{Cr})$ ($A = $ Pd and Pt), which also correlates with the fact that W and Cr alloys have the most and least amounts of total charge transfer, respectively. However, from the amount of total charge transfer, it is not immediately obvious why $\varepsilon_{\mathrm{CE}}(A_8\mathrm{V})$ is the lowest for $A=$Pd and Pt.

(iii) For a fixed B atom, $\varepsilon_{\mathrm{CE}}(Pt_8B) < \varepsilon_{\mathrm{CE}}(Pd_8B)$, and this is at first sight opposite to the argument of correlating $\varepsilon_{\mathrm{CE}}$ with charge transfer, since there is more charge being transferred in the Pd than the Pt alloy. This seeming paradox can be explained by the fact that elemental Pt has one of the deepest s states (a relativistic effect) among all transition metals: Its measured[30] atomic s ionization potential (9.0 eV) is only exceeded by Ir (9.1 eV) and Au (9.2 eV), and hence, a similar amount of charge transfer into the Pt s state would lower the band energy much more than the similar Pd systems, and thus the total energy of the Pt alloy is much lower than that of Pd. Indeed, the amount of s electrons lost from the B atom is larger in the Pt alloy than in the corresponding Pd alloy. This relativistic lowering of the s state in Pt is also responsible[31,32] for the observed $L1_0$ ordering in Ni-Pt, for which the conventional d-band-filling tight-binding arguments[33-35] would suggest phase separation rather than ordering. The enhanced stability of Pt alloys relative to Pd alloys has also been discussed previously by Wolverton et al.[16]

TABLE V. The table shows the amount of "charge transfer," defined as the difference of the amount of charge within the muffin-tin radii in the A_8B phase and in the pure fcc structure at the same lattice constant a (close to the calculated lattice constants). We decompose $\delta Q_l^{\mathrm{MT}} == Q_l^{\mathrm{MT}}(A_8B) - Q_l^{\mathrm{MT}}(\mathrm{fcc})$ into different l characters, i.e., s, p, d, and total charge. We give the average δQ for the A atoms (there are two distinct types of A atoms in the unit cell).

δQ_l^{MT}	Ni[a]	Ni[b]	Pd[c]	Pd[d]	Pd[e]	Pd[f]	Pt[g]	Pt[h]	Pt[i]	Pt[j]
s	0.016	0.012	0.015	0.011	0.019	0.019	0.013	0.013	0.016	0.015
p	0.017	0.016	0.011	0.009	0.021	0.027	0.002	0.001	0.010	0.016
d	0.016	0.006	−0.002	−0.008	0.002	0.006	−0.002	−0.015	0.007	0.014
Total	0.049	0.035	0.020	0.008	0.041	0.052	0.009	−0.008	0.032	0.043
δQ_l^{MT}	V[a]	Cr[b]	V[c]	Cr[d]	Mo[e]	W[f]	V[g]	Cr[h]	Mo[i]	W[j]
s	−0.076	−0.057	−0.057	−0.030	−0.055	−0.046	−0.065	−0.040	−0.061	−0.060
p	−0.038	−0.240	−0.036	−0.023	−0.050	−0.090	0.004	0.007	−0.012	−0.055
d	−0.356	−0.180	−0.144	−0.040	−0.331	−0.393	−0.083	0.015	−0.257	−0.300
Total	−0.465	−0.296	−0.214	−0.082	−0.435	−0.531	−0.111	−0.004	−0.313	−0.402

[a]Calculated at $a = 3.466$ Å, the muffin-tin radii are $R_{\mathrm{MT}}^{\mathrm{Ni}} = 1.164$ Å and $R_{\mathrm{MT}}^{\mathrm{V}} = 1.217$ Å.
[b]Calculated at $a = 3.469$ Å, $R_{\mathrm{MT}}^{\mathrm{Ni}} = 1.164$ Å and $R_{\mathrm{MT}}^{\mathrm{Cr}} = 1.164$ Å.
[c]Calculated at $a = 3.852$ Å, $R_{\mathrm{MT}}^{\mathrm{Pd}} = 1.270$ Å and $R_{\mathrm{MT}}^{\mathrm{V}} = 1.270$ Å.
[d]Calculated at $a = 3.851$ Å, $R_{\mathrm{MT}}^{\mathrm{Pd}} = 1.270$ Å and $R_{\mathrm{MT}}^{\mathrm{Cr}} = 1.164$ Å.
[e]Calculated at $a = 3.890$ Å, $R_{\mathrm{MT}}^{\mathrm{Pd}} = 1.270$ Å and $R_{\mathrm{MT}}^{\mathrm{Mo}} = 1.270$ Å.
[f]Calculated at $a = 3.895$ Å, $R_{\mathrm{MT}}^{\mathrm{Pd}} = 1.270$ Å and $R_{\mathrm{MT}}^{\mathrm{W}} = 1.270$ Å.
[g]Calculated at $a = 3.914$ Å, $R_{\mathrm{MT}}^{\mathrm{Pt}} = 1.270$ Å and $R_{\mathrm{MT}}^{\mathrm{V}} = 1.270$ Å.
[h]Calculated at $a = 3.896$ Å, $R_{\mathrm{MT}}^{\mathrm{Pt}} = 1.270$ Å and $R_{\mathrm{MT}}^{\mathrm{Cr}} = 1.164$ Å.
[i]Calculated at $a = 3.937$ Å, $R_{\mathrm{MT}}^{\mathrm{Pt}} = 1.270$ Å and $R_{\mathrm{MT}}^{\mathrm{Mo}} = 1.270$ Å.
[j]Calculated at $a = 3.942$ Å, $R_{\mathrm{MT}}^{\mathrm{Pt}} = 1.270$ Å and $R_{\mathrm{MT}}^{\mathrm{W}} = 1.270$ Å.

Figure 3 illustrates the LAPW-calculated, total density of states (DOS) for Ni_8V, Pd_8V, and Pt_8V. The overall shapes of these densities of states resemble the DOS of the respective elements (Ni, Pd, and Pt): Ni_8V and Pt_8V have the smallest and largest bandwidth, respectively, while Pt_8V has the deepest low-lying s states (down to -10 eV below E_F) and Pd_8V has the most shallow s state (-8 eV below E_F). The Fermi energies are moved inward towards the higher binding energy, as vanadium has only five valence electrons rather than ten in Ni, Pd, and Pt. The densities of states at the Fermi energy $N(E_F)$ are 1.50, 1.05, 1.18 states/atom eV for Ni_8V, Pd_8V, and Pt_8V, respectively.

VIII. ELECTRON-PHONON COUPLINGS AND SUPERCONDUCTIVITY

We are not aware of any experimental studies of superconductivity for the A_8B compounds, and so it is particularly worthwhile to make theoretical estimates of whether or not they are expected to be interesting superconductors. The coupling strength for superconductivity, λ, can be written as

$$\lambda = \sum_a \left(\frac{\eta_a}{M_a}\right) \bigg/ \langle\omega^2\rangle , \qquad (10)$$

with M_a the mass of atom a in the unit cell, η_a the McMillan-Hopfield electron-phonon coupling factor, and $\langle\omega^2\rangle$ is a mean-squared average phonon frequency, weighted by the relative coupling strength of each phonon
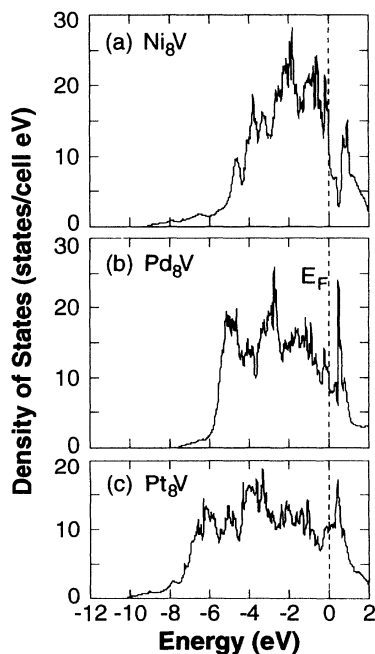
FIG. 3. The calculated total density of states for (a) Ni_8V, (b) Pd_8V, and (c) Pt_8V at lattice parameters of 3.466 Å, 3.852 Å, and 3.914 Å, respectively. The energy zeros are set at the respective Fermi energies.

mode. The value of $\langle\omega^2\rangle$ must be estimated for these systems. For good metals such as these, a good approximation for determining the η_a is made by using the rigid-muffin-tin approximation (RMTA) method of Gaspari and Gyorffy.[36,37] The inputs into the RMTA are the muffin-tinized potentials of each component, and the total and site-angular-momentum-decomposed densities of states, all available from our calculations. The results for η_a are given in Table VI. We see from Table VI that the η_a values for V are small, much smaller than for elemental, metallic V, and the η_a values for either of Ni, Pd, or Pt are also modest compared to those of good superconductors, too.[38] Using estimates for $\langle\omega^2\rangle$ ranging from 20^2 to 50^2 meV^2, we find λ is predicted to be less than 0.3 for all three compounds. Using the McMillan equation to estimate the superconducting transition temperature, we find T_c should be very low, 1 K or less, or nonexistent, for these A_8V compounds. This is largely related to the modest $N(E_F)$ values for the A_8B materials compared to good transition-metal superconductors.

IX. PREVIOUS THEORETICAL EFFORTS ON THE A_8B SYSTEMS

There are several previous theoretical efforts[15,16,39,40] which examined the stability of some of the A_8B compounds. Using the generalized perturbation method (GPM) based on the coherent potential approximation (CPA), Turchi et al.[39] extracted effective pair interactions (perturbated around a disordered medium) up to the fourth nearest neighbors and thus directly obtained a negative ordering energy [the energy difference between an ordered phase σ and the disordered phase at the same composition, i.e., $\Delta E_{ord} = \Delta H(\sigma) - \Delta E_{mix}(x)$] for Pd_8V in the Pt_8Ti-type structure. Because of the perturbative nature of the GPM, these authors did not explicitly calculate the mixing energy $\Delta E_{mix}(x)$ of the disordered phase, and so did not fully address the stabilities of competing phases. Nevertheless, they suggest that the Pd_8V in the

TABLE VI. Entries are the McMillan-Hopfield electron-phonon parameters, η_a, discussed in the text, in units of $eV/Å^2$. The listed values are per atom for each species (note that there are two different sites for Ni, Pd, or Pt, each representing four equivalent atoms — the full unit cell contribution from each of these are 4 times the listed values).

	η_a A_8B compounds	η_a Pure metals
Ni(1)	0.18	1.76
Ni(2)	0.20	1.76
V	0.03	6.89
Pd(1)	0.30	1.99
Pd(2)	0.22	1.99
V	0.06	6.89
Pt(1)	0.54	Not available
Pt(2)	0.39	Not available
V	0.10	6.89

Pt_8Ti-type structure is stable.

Recently Wolverton et al.[16] studied the stability of a number of binary intermetallic systems (including Pd-Ti, Pd-V, Pt-Ti, and Pt-V) in fcc-based structures (note that at equilibrium V and Ti have the bcc and hcp structures, respectively). They obtained effective cluster interactions (including pairs, triplets, and quadruplets) based on a tight-binding linear muffin-tin orbital (TB-LMTO) Hamiltonian using the direct average technique, and they subsequently searched the ground states of these alloy systems using the linear programming technique. They found that Pd_8V, Pt_8Ti, and Pt_8V in the Pt_8Ti-type structure are metastable: i.e., these phases have the lowest energy at $x = \frac{1}{9}$, but their formation energies are slightly *above* the tie lines connecting the predicted neighboring ground states and end points (Pd or Pt). The discrepancies with the present results are possibly due to their use of the more approximate TB LMTO versus our more accurate LAPW results (see below).

Fernando et al.[40] calculated the $T = 0$ K formation energy for Pt-Ti systems in a number of ordered structures using the full-potential linear Slater-type orbital (LASTO) method. They found that Pt_8Ti is stable among the set of structures that they calculated. They further emphasized the importance of using a full-potential method in calculating the formation energy: The difference in the calculated ΔH between a muffin-tin and a full-potential treatment was found to be substantial, as much as 250 meV/atom for some structures. Note that the above-mentioned CPA-GPM (Ref. 39) and TB-LMTO direct configurational averaging (Ref. 17) methods used spherical potentials, while the present study (as well as Ref. 40) employs a full-potential method.

Using the Connolly-Williams[41] cluster expansion (CE) approach, Lu and Zunger[15] mapped the formation energy of ~ 20 structures (calculated using the full potential LAPW method) onto Ising-like effective cluster interactions (including pairs, triplets, and quadruplets) for the Ni-V system. They then subjected the resulting cluster interactions to a Monte Carlo simulated annealing treatment, and obtained low-temperature ground states and high-temperature short-range order parameters. For $x = \frac{1}{9}$, the cluster expansion failed to find the experimentally observed Pt_8Ti-type structure as the ground state despite the fact that our present direct LAPW calculations find the Pt_8Ti-type structure to be the lowest-energy structure at this composition (note that the CE correctly predicts the DO_{22} and $MoPt_2$ to be the ground states at $x = \frac{1}{4}$ and $x = \frac{1}{3}$, respectively). This reflects a fitting error in the cluster expansion: While LAPW gives a value of $\Delta H_{LAPW} = -189.4$ meV/atom for Ni_8V, the cluster expansion gives $\Delta H_{CE} = -175.5$ meV/atom. In fact, at this composition ($x = \frac{1}{9}$) the cluster expansion places another structure lower in energy ($\Delta H_{CE} = -189.2$ meV/atom) than the Pt_8Ti structure. The di-

Stable A_8B phases

	V	Cr	Mo	W
Ni	√	!	√	!
Pd	√		√	√
Pt	√	!	!	!

FIG. 4. This figure summarizes the finding of this work: All these A_8B phases (except Pd_8Cr), where A = Ni, Pd, and Pt, while B = V, Cr, Mo, and W are found to be stable thermodynamically (marked by the exclamation mark !); i.e., the calculated $\Delta H(A_8B) < 0$ and $\Delta H(A_8B)$ lie below the tie line between neighboring known or suspected ground states. We also show the experimentally identified A_8B phases by the $\sqrt{}$ symbol.

rect LAPW-calculated $\Delta H_{LAPW} = -189.4$ meV/atom for the Pt_8Ti structure is actually ~ 50 meV/atom *below* the tie line connecting the known ground state DO_{22} at $x = \frac{1}{4}$ and the end point $x = 0$. Thus, while LAPW predicts the Pt_8Ti-type structure to be the lowest energy at $x = \frac{1}{9}$, the ~ 14 meV/atom error of the CE obscures this result in a ground-state search.

X. SUMMARY

The main findings of this work can be summarized by Fig. 4: All of the studied A_8B phases (except Pd_8Cr), where A = Ni, Pd, and Pt, and B = V, Cr, Mo, and W, are stable at $T = 0$ (indicated by the exclamation marks); i.e., the LAPW-calculated formation energies $\Delta H(A_8B)$ are negative. Hence, they are stable with respect to phase separation into their equilibrium constituents A and B. Furthermore, the calculated values of $\Delta H(A_8B)$ lie below the tie line between neighboring known or suspected ground states, and hence, they are also stable with respect to phase separation into neighboring equilibrium ground states. The experimentally identified A_8B systems (indicated by the $\sqrt{}$ symbols in Fig. 4) are indeed found to be stable theoretically. These A_8B phases appears to be the true low-temperature ground states for these alloy systems. We calculate their electron-phonon interactions. We conclude that these materials are unlikely to be superconductors.

ACKNOWLEDGMENTS

[1] For an experimental review see A. J. Ardell, in *Metallic Alloys: Experimental and Theoretical Perspectives*, Vol. 256 of *NATO Advanced Study Institute: Series E*, edited by J. S. Faulkner and R. G. Jordan (Kluwer Academic, Dordrecht, 1994).

[2] P. Pietokowsky, Nature **206**, 291 (1965).

[3] P. Krautwasser, S. Bhan, and K. Schubert, Z. Metallkd. **59**, 724 (1968).

[4] W. E. Quist, C. J. van der Wekken, R. Taggart, and D. H. Polonis, Trans. Met. Soc. AIME **245**, 345 (1969).

[5] J. M. Lars, R. Taggart, and D. H. Polonis, Metall. Trans. **1**, 485 (1970).

[6] H. A. Moreen, R. Taggart, and D. H. Polonis, J. Mater. Sci. **6**, 1425 (1971).

[7] L. Weaver and A. J. Ardell, Scr. Metall. **14**, 765 (1980).

[8] A. J. Ardell and K. Janghorban, in *Phase Transformations During Irradiation*, edited by F. V. Nolfi (Applied Science, London, 1982), p. 291.

[9] D. Schryvers, J. Van Landuyt, and S. Amelinckx, Mater. Res. Bull. **18**, 1369 (1983).

[10] J. Mayer and K. Urban, Phys. Status Solidi A **90**, 469 (1985).

[11] M. S. Mostafa and A. J. Ardell, Mater. Lett. **3**, 67 (1987).

[12] J. Cheng and A. J. Ardell, J. Less-Common Met. **141**, 45 (1988).

[13] Whether a structure will be observed experimentally depends on many other factors; for example, the order-disorder transition temperature should be sufficiently high, and the elastic constants C_{ij} of the structure should satisfy certain stability constraints. See for example, J. Chen, L. L. Boyer, H. Krakauer, and M. J. Mehl, Phys. Rev. B **37**, 3295 (1988).

[14] P. Hohenberg and W. Kohn, Phys. Rev. **136**, B864 (1964); W. Kohn and L. J. Sham, *ibid.* **140**, A1133 (1965).

[15] Z. W. Lu and A. Zunger, Phys. Rev. B (to be published).

[16] C. Wolverton, G. Ceder, D. de Fontaine, and H. Dreyssé, Phys. Rev. B **48**, 726 (1993).

[17] E. Wigner, Phys. Rev. **46**, 1002 (1934).

[18] O. K. Andersen, Phys. Rev. B **12**, 3060 (1975); E. Wimmer, H. Krakauer, M. Weinert, and A. J. Freeman, *ibid.* **24**, 864 (1981); D. R. Hamann, Phys. Rev. Lett. **42**, 662 (1979); S.-H. Wei and H. Krakauer, *ibid.* **55**, 1200 (1985); S.-H. Wei, H. Krakauer, and M. Weinert, Phys. Rev. B **32**, 7792 (1985).

[19] H. J. Monkhorst and J. D. Pack, Phys. Rev. B **13**, 5188 (1976).

[20] D. Murnaghan, Proc. Natl. Acad. Sci. USA **30**, 244 (1944).

[21] The displacement of the unit cell vectors ("cell external relaxations") and symmetry-allowed atomic displacements within the unit cell ("cell-internal relaxations") will always lower the energy. However, this energy lowering appears to be fairly small for the compounds considered here. For example, in the case of Ni-V, the lattice relaxation lowers the formation energy of the DO_{22} structure (Ni$_3$V) from -313.3 to -315.2 meV/atom and the Pt$_2$Mo-type structure (Ni$_2$V) from -301.9 to -302.3 meV/atom.

[22] P. Villar and L. D. Calvert, *Pearson's Handbook of Crys-tallographic Data for Intermetallic Phases*, 2nd ed. (ASM International, Materials Park, OH, 1991).

[23] C. Kittle, *Introduction to Solid State Physics*, 6th ed. (Wiley, New York, 1986).

[24] *Binary Alloy Phase Diagrams*, edited by T. B. Massalski (ASM international, Materials Park, OH, 1991), Vols. 1, 2, and 3.

[25] The DO_{22} structures are characterized by the Lifshitz point of $\langle 1\frac{1}{2}0\rangle$, the observed high-temperature diffused scattering (Refs. 26–28), and show different behaviors for these vanadium compounds; i.e., while Ni$_3$V shows diffused scattering intensity peaks at the $W = \langle 1\frac{1}{2}0\rangle$ points, the Pd$_3$V and Pt$_3$V show peaks at the $X = \langle 100\rangle$ points, contrary to the conventional mean-field expectations. See Refs. 26 and 29 for explanations.

[26] F. Solal, R. Caudron, F. Ducastelle, A. Finel, and A. Loiseau, Phys. Rev. Lett. **58**, 2245 (1987).

[27] R. Caudron, M. Sarfati, M. Barrachin, A. Finel, F. Ducastelle, and F. Solal, J. Phys. I France **2**, 1145 (1992).

[28] D. Schryvers and S. Amelinckx, Acta Metall. **34**, 43 (1986).

[29] C. Wolverton, A. Zunger, and Z. W. Lu, Phys. Rev. B **49**, 16 058 (1994).

[30] L. H. Ahren, *Ionization Potentials* (Pergamon, Oxford, 1983).

[31] Z. W. Lu, S.-H. Wei, and A. Zunger, Phys. Rev. Lett **66**, 1753 (1991); **68**, 1961 (1992).

[32] Z. W. Lu, S.-H. Wei, and A. Zunger, Europhys. Lett. **21**, 221 (1993).

[33] J. Van Der Rest, F. Gautier, and F. Brouers, J. Phys. F **5**, 2283 (1975); M. Cyrot and F. Cyrot-Lackmann, *ibid.* **6**, 2257 (1976); M. Sluiter, P. Turchi, and D. de Fontaine, *ibid.* **17**, 2163 (1987); G. Treglia and F. Ducastelle, *ibid.* **17**, 1935 (1987).

[34] D. G. Pettifor, Phys. Rev. Lett. **42**, 846 (1979).

[35] A. Bieber and F. Gautier, Acta Metall. **34**, 2291 (1986).

[36] G. D. Gaspari and B. L. Gyorffy, Phys. Rev. Lett. **29**, 801 (1972).

[37] B. M. Klein and W. E. Pickett, in *Superconductivity in d- and f-Band Metals, 1982*, edited by W. Buckel and W. Weber (Kernforschungszentrum Karlsruhe GmbH, Karlsruhe, 1982), p. 477.

[38] D. A. Papaconstantopoulos *et al.*, Phys. Rev. B **15**, 4221 (1977).

[39] P. E. A. Turchi, G. M. Stocks, W. H. Butler, D. M. Nicholson, and A. Gonis, Phys. Rev. B **37**, 5982 (1988).

[40] G. W. Fernando, R. E. Watson, and M. Weinert, Phys. Rev. B **45**, 8233 (1992).

[41] J. W. D. Connolly and A. R. Williams, Phys. Rev. B **27**, 5169 (1983).